Biomed Microdevices (2012) 14:401–407
DOI 10.1007/s10544-011-9616-5

Immunocapture of prostate cancer cells by use of anti-PSMA antibodies in microdevices

Steven M. Santana · He Liu · Neil H. Bander · Jason P. Gleghorn · Brian J. Kirby

Published online: 6 December 2011

Abstract Patients suffering from cancer can shed tumor cells into the bloodstream, leading to one of the most important mechanisms of metastasis. As such, the capture of these cells is of great interest. Circulating tumor cells are typically extracted from circulation through positive selection with the epithelial cell-adhesion molecule (EpCAM), leading to currently unknown biases when cells are undergoing epithelial-to-mesenchymal transition. For prostate cancer, prostate-specific membrane antigen (PSMA) presents a compelling target for immunocapture, as PSMA levels increase in higher-grade cancers and metastatic disease and are specific to the prostate epithelium. This study uses monoclonal antibodies J591 and J415—antibodies that are highly specific for intact extracellular domains of PSMA on live cells—in microfluidic devices for the capture of LNCaPs, a PSMA-expressing immortalized prostate cancer cell line, over a range of concentrations and shear stresses relevant to immunocapture. Our results show that J591 outperforms J415 and a mix of the two for prostate cancer capture, and that capture performance saturates following incubation with antibody concentrations of 10 micrograms per milliliter.

Keywords CTC · Microfluidic · PSMA · J591 · Circulating tumor cell · Prostate cancer

Abbreviations

PCa	Prostate Cancer
PCTC	Prostate Circulating Tumor Cell
CTC	Circulating Tumor Cell
EpCAM	Epithelial Cell Adhesion Molecule
EMT	Epithelial-to-Mesenchymal Transition
PSMA	Prostate Specific Membrane Antigen
CRPC	Castrate Resistant Prostate Cancer

1 Introduction

Patients suffering from metastatic prostate cancer (PCa) often shed tumor cells, called prostate circulating tumor cells (PCTCs), into the bloodstream (Allard et al. 2004; Danila et al. 2007). Although these PCTCs are rare and are

S. M. Santana · B. J. Kirby
Sibley School of Mechanical and Aerospace Engineering,
Cornell University,
245 Upson Hall,
Ithaca, NY 14853, USA

S. M. Santana
e-mail: sms492@cornell.edu
URL: http://www.kirbyresearch.com/santana

H. Liu · N. H. Bander
Laboratory of Urological Oncology,
Weill Medical College of Cornell University,
1300 York Avenue, E-300,
New York, NY 10065, USA

H. Liu
e-mail: hliu@med.cornell.edu

N. H. Bander
e-mail: nhbander@med.cornell.edu
URL: http://weill.cornell.edu/research/researcher/neilhbander

J. P. Gleghorn
School of Engineering and Applied Science, Department of Chemical and Biological Engineering, Princeton University,
E-Quad A220, 59 Olden Street,
Princeton, NJ 08544, USA
e-mail: gleghorn@princeton.edu

B. J. Kirby (✉)
Sibley School of Mechanical and Aerospace Engineering,
Cornell University,
238 Upson Hall,
Ithaca, NY 14853, USA
e-mail: kirby@cornell.edu
URL: http://www.kirbylab.com/

outnumbered by as much as 10^9 hematologic cells per PCTC in blood, it is believed that these circulating tumor cells (CTCs) contribute to metastatic progression (Krivacic et al. 2004). PCTC enumeration has been shown clinically to be a valid prognostic indicator of patient survival (Danila et al. 2007; de Bono et al. 2008; Scher et al. 2009). The capture of PCTCs may enable early clinical assessment of metastatic processes and chemotherapeutic responses, as well as genetic and pharmacological evaluation of cancer cells.

CTC isolation is inhibited by the uncertainty in defining appropriate enrichment schemes. Circulating nucleated cells (DAPI+) that show evidence of an epithelial history (EpCAM+, cytokeratin+) and are distinct (CD45-) from leukocytes are often classified as originating from the primary tumor and being related to metastasis (Allard et al. 2004; Coumans et al. 2010). Use of these identifying characteristics is supported by statistical observations that high counts of CTCs defined in this fashion correlate with poor prognosis (Coumans et al. 2010). CTCs are most commonly extracted from circulation through an enrichment process by positive selection with EpCAM (also called CD326), a pan-epithelial marker (Nagrath et al. 2007; Shaffer et al. 2007; Olmos et al. 2009; Stott et al. 2010a,b); this mechanism is employed by the CellSearch™ system and by other immunocapture systems (Danila et al. 2007; de Bono et al. 2008; Olmos et al. 2009; Pantel and Alix-Panabières 2010; Riethdorf and Pantel 2010; Pratt et al. 2011).

EpCAM has often been selected as the target transmembrane protein in immunocapture systems because of the epithelial origin of the cells of interest, but this approach may introduce biases due to the dynamic nature of EpCAM expression in circulating cells (Pantel and Alix-Panabières 2010). Importantly, patients with solid tumors and high CTC counts (as measured following EpCAM enrichment) have poor prognoses (Moreno et al. 2005; Danila et al. 2007; Cohen et al. 2008; de Bono et al. 2008; Olmos et al. 2009; Coumans et al. 2010). Whereas EpCAM has been reported to correlate with invasiveness (Shiah et al. 2008), indicate oncogenic potential (Munz et al. 2009), and be upregulated and correlate with proliferation in cell lines (Gostner et al. 2011), the role of EpCAM in metastatic cancer is unclear. An important cellular phenotype change, epithelial-to-mesenchymal transition (EMT), characteristic of many invading cancer cells, results in a cell's loss of epithelial characteristics. This transition may cause some populations of CTCs to avoid extraction through epithelial-based (anti-EpCAM) capture techniques as EpCAM expression (Maheswaran and Haber 2010; Pantel and Alix-Panabières 2010) does not correlate with EMT markers (Mego et al. 2009). Furthermore, markers expressed after EMT may be more important in predicting cancer progression as they contribute to metastatic potential (Gradilone et al. 2011). EMT has been reported to increase a cell's ability to become invasive, perhaps leading to a higher probability of tumorigenicity; thus, cells more aggressive in the generation of new tumors might not be isolated by EpCAM enrichment (Pantel and Alix-Panabières 2010).

In prostate tissues, including PCTCs, prostate-specific membrane antigen (PSMA; also known as: folate hydrolase 1 or glutamate carboxypeptidase II), a type II transmembrane metallopeptidase, is a well-established ligand that is accessible to antibodies (Liu et al. 1997; Chang et al. 1999b; Bander et al. 2003; Davis et al. 2005). Virtually all prostate cancer primary tumors express PSMA (Wright et al. 1995; Murphy et al. 1998; Kusumi et al. 2008; Ananias et al. 2009; Mannweiler et al. 2009), whereas PSMA is only minimally expressed in prostate vascular endothelium of benign tissue (Chang et al. 1999a). PSMA levels increase progressively in higher-grade cancers, metastatic disease, hormone-refractory cancer, progressing cancer, and cancers exhibiting rising blood PSA following prostatectomy (Israeli et al. 1994a; Wright et al. 1995; Wright et al. 1996; Sweat et al. 1998; Ross et al. 2003; Perner et al. 2007; Minner et al. 2011). Thus, anti-PSMA immunocapture is likely to capture circulating prostate cells independent of when cells undergo EMT.

Monoclonal antibodies J591 and J415, both of which are highly specific for PSMA (Liu et al. 1997), were conjugated to the surfaces of microfluidic devices for the capture of a PSMA-expressing prostate cancer cell line, LNCaP. We have previously reported high-efficiency and high-purity capture of PCTCs from CRPC patient blood samples, as well as LNCaP cells, with monoclonal antibody J591 (Gleghorn et al. 2010). Here, we report the relationship between the concentration of antibody in solution during functionalization and the final surface conjugated ligand density, the capture performance of monoclonal anti-PSMA antibodies for cell isolation over a range of concentrations and shear stresses within microfluidic devices, and the competition between multiple PSMA antibodies used simultaneously.

2 Experimental

2.1 Materials

LNCaP cells, a PSMA-expressing prostate cancer cell line, were purchased from the American Type Culture Collection (ATCC; Manassass, VA). A Fusion-100 syringe pump was purchased from Chemyx (Stafford, TX). Corning CellBIND surface 75 cm^2 culture flasks were purchased from ThermoFisher Scientific (Waltham, MA). Sylgard® 184 Silicone Elastomer Kit (polydimethylsiloxane, PDMS), was purchased from Dow-Corning (Midland, MI). Fetal bovine serum (FBS) was purchased from Gemini Bio-products (West Sacramento, CA). The plasma cleaner was purchased from Harrick Plasma (Ithaca, NY). The hemacytometer was

purchased from Hausser Scientific (Hanshaw, PA). Dulbecco's Phosphate-Buffered Saline (PBS) solution, RPMI-1640 cell culture media, antibiotic-antimycotic solution (Penicillin-Streptomycin), and trypan blue solution were purchased from Mediatech (Manassass, VA). The Eclipse TE2000U inverted microscope was purchased from Nikon (Melville, NY). (3-Mercaptopropyl) trimethoxysilane (MPTMS), 200 proof anhydrous ethanol (EtOH), Dimethyl Sulfoxide (DMSO), Bovine Serum Albumin (BSA), Trypsin-EDTA solution, and 1,1,2,2 tetrahydroperfluorooctyltrichlorosilane were purchased from Sigma-Aldrich (St. Louis, MO). Harris Uni-Core™, tip diameter 0.50 mm, was purchased from Ted Pella (Redding, CA). (N-[γ-maleimidobutyryloxy]succinimide ester) (GMBS), NeutrAvidin Protein, EZ-Link NHS-LC-LC-Biotin, Goat Anti-Mouse IgG DyLight™ 594 secondary antibody, Reacti-Bind™ NeutrAvidin™ Coated 96-Well Black Plates, Monoclonal biotinylated murine antibodies J591 and J415 were provided by Dr. Neil Bander. A Synergy HT BioTek plate reader was used for the immunofluorescence assays.

2.2 Microdevice design

Examining microfluidic devices that make use of the fluid mechanics and geometries within becomes difficult as the topologies and materials make characterization of cell adhesion difficult to quantify. Hele-Shaw flow cells, high aspect ratio devices that exhibit Stokes flow between two flat plates, provide a simple and useful platform through which to tune flow characteristics for the capture of rare cells. A Hele-Shaw flow cell facilitates analysis of defined flow characteristics, specifically shear stress, because the fluid velocity field variations in the plane of the device are often amenable to analytical solution. These devices facilitate simple visualization and mapping of shear stresses. Cell capture within the microfluidic device depends on the number of interactions a cell will have with immunocoated surfaces as well as the contributions of shear stress (Murthy et al. 2004; Gleghorn et al. 2010). Preferable flow parameters constitute flow conditions that maximize target cell viability and capture efficiency as measured by the total number of viable captured cells as compared to those present in the original sample, and purity, which is the percent of isolated cells that match the target population. The device geometry, shown with images of captured cells, is shown in Fig. 1 (Usami et al. 1993; Murthy et al. 2004). This device design emulates the analytical solution for potential stagnation flow. This design maintains the linear decrease in shear stress predicted by the analytical solution along approximately half of its length. Deviations from the analytical solution result from experimentally implemented inlets, outlets, and impenetrable boundaries. Using flow through this

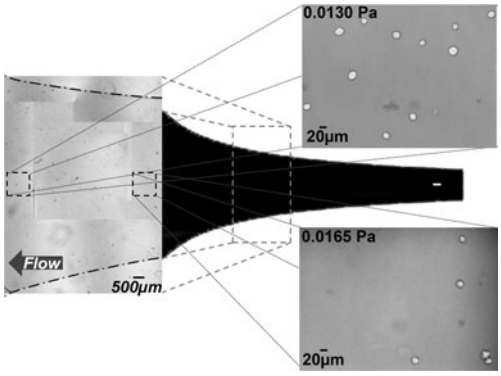

Fig. 1 The Hele-Shaw flow cell geometry used for these experiments is defined by the streamlines of a stagnation point flow. This form generates a linear variation in shear stress along the device's centerline. Representative images are shown of observation fields with cells immobilized on a J591-terminated surface. The locations indicated on the image correspond to local shear stresses of 0.0165 Pa and 0.0130 Pa. The listed shear stress values correspond to a device with dimensions of: depth 48 μm, length 50 mm, inlet width 5 mm; for a volumetric flow rate of 0.2 mL/hr; with PBS. The shear stresses examined in these studies ranged from 0.008 Pa to 0.024 Pa

device, each experimental run characterizes cell adhesion over a wide range of shear stresses, corresponding to those experienced within microfluidic immunocapture devices (Murthy et al. 2004; Sin et al. 2005; Gleghorn et al. 2010).

2.3 Microdevice fabrication

Microfluidic device masters were created in the Cornell Nanofabrication Facility (CNF) at Cornell University using standard photolithography techniques. SU-8 Hele-Shaw device masters were fabricated by spin-coating silicon wafers with SU-8 to create a film thickness of 48 microns. The photoresist was patterned and coated with 1,1,2,2 tetrahydroperfluorooctyltrichlorosilane, to create a non-stick coating.

This master was used to construct PDMS and glass devices. PDMS was prepared using a standard Sylgard® 184 Elastomer kit and a 5:1 ratio of the elastomer base to the curing agent and baked in a vacuum oven for a period of 8 h at 60°C. PDMS was removed from the master, inlet and outlet holes were punched and the patterned PDMS was cleaned using an acetone and isopropyl alcohol (IPA). Glass was prepared using a standard acid (HCl)—base (NaOH) wash followed by an acetone and IPA rinse. Both the glass and the PDMS were dried under a nitrogen stream. The PDMS and glass components were plasma cleaned for 40 s, bonded together and baked at 60° C for 4 h.

2.4 Microdevice functionalization

All capture experiments described herein are conducted with monoclonal antibodies J591 and J415; both have a high binding avidity to and specificity for epitopes on the

extracellular PSMA domain and minimal nonspecific binding with PSMA-negative cells (Liu et al. 1997). The glass surfaces of the Hele-Shaw microdevices were functionalized to immobilize these antibodies. Antibody functionalization of an amine-terminated surface was accomplished through a two-step process by use of incubation in 4% (v/v) MPTMS in EtOH solution for 30 min followed by a 20 minute incubation with a 1 mM GMBS in EtOH solution. Next, a layer of NeutrAvidin was covalently attached to the surface by incubating the surface for 60 min with 25 micrograms of NeutrAvidin per milliliter of PBS. Finally, the biotinylated monoclonal antibody was immobilized on the surface via the biotin-NeutrAvidin bond (Liu et al. 1997; Kirby et al. 2003; Gleghorn et al. 2010). Devices were stored before use in a 1% (m/v) BSA in PBS solution for up to two hours.

2.5 Cell maintenance

All capture experiments were conducted with LNCaP cells, an immortalized prostate cancer cell line derived from a human prostate adenocarcinoma that is known to express PSMA (Wright et al. 1996; Chang et al. 1999b). This cell line was selected to understand the capture performance in a population completely expressing the target epitope. LNCaP cells were cultured in T75 flasks at 37°C in a 5% CO_2, humidified environment. Cells were cultured in RPMI-1640 supplemented with 10% FBS and 1% Penicillin-Streptomycin. To prepare cells for experiments, they were removed from the culture flasks and resuspended in 1 mM EDTA in 1% (m/v) BSA in PBS for a cell suspension density of 3×10^5 LNCaP cells/mL.

2.6 Immunofluorescence assay

To quantify biotinylated-antibody adhesion to and saturation on the surface an immunofluorescence assay was completed. A series of solutions with different J591 mAb concentrations (0.25–160 μg/mL) were prepared via serial dilution. 100 microliters of each dilution was incubated on wells of a NeutrAvidin-coated 96-well plate for 1 h. Following incubation, all wells were washed with PBS and subsequently incubated with a 1% (m/v) BSA in PBS solution as a blocking buffer. The blocking buffer was removed and the wells were washed with PBS. Finally, a fluorophore-conjugated murine secondary antibody in PBS was incubated in the antibody-conjugated wells for 1 h. After incubation, all wells were washed with PBS and read by a plate reader.

2.7 Capture experiments

To simulate the local shear stress experienced by cells within immunocapture microdevices, a cell suspension was flowed through the Hele-Shaw microdevices at a rate of 0.2 mL/hr using a Chemyx Fusion 100 syringe pump. Subsequently, a solution of 1% (m/v) BSA in PBS with 1% (v/v) Trypan blue was flowed through the chamber at 0.2 mL/hr for 15 min to wash away any non-adhered cells. Images were taken at a 20× magnification under bright field at a series of predetermined observation sites along the length of the device. For the capture experiments, cell count values were collected for 14 unique shear stress regions with at least eight repetitions. For all shear stresses, the reported value corresponds to the shear stress at the wall in the center of the imaged area. The cell counts reported in each graph correspond to the number of cells imaged in a 1 mm^2 region at the central axis of the Hele-Shaw flow cell associated with each reported shear stress. In comparing the performance of antibodies, a two-way ANOVA and Tukey post hoc test ($\alpha=0.05$) were completed analyzing both shear stress and antibody selection as influencing factors on the number of cells isolated in each observed region.

3 Results

To measure the effect of antibody incubating solution concentration on bound antibody, we performed an immunofluorescence assay on J591 antibody with incubating solutions of concentration ranging from 0.25–160 μg/mL. Antibody binding, as quantified by fluorescence from a functionalized secondary antibody, shown in Fig. 2, indicates antibody

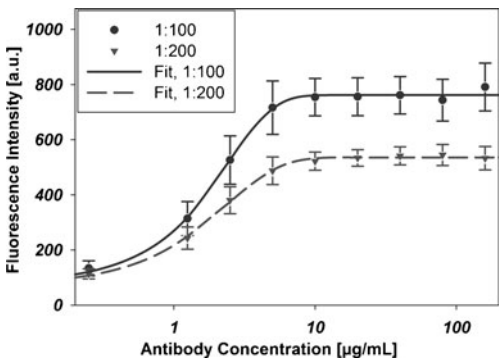

Fig. 2 Immunofluorescence data indicate surface coverage of immobilized biotinylated-J591 on a NeutrAvidin-coated substrate. Antibody concentrations represent the concentration of antibody in the incubating solution in micrograms per milliliter. All J591 dilutions were prepared from a stock solution of concentration 2 mg/mL. Unique curves indicate the dilution of the stock fluorophore-conjugated murine secondary antibody solution (2 mg/mL) to PBS used to stain the surface. Error bars represent standard error of the mean, all data points are representative of six repetitions ($n=6$). Each curve was fit with a 4-parameter Langmuir adsorption isotherm. $EC50_{1:100}=1.5636$ μg/mL, $EC50_{1:200}=1.3848$ μg/mL

saturation on the surface for an incubating solution concentration of 10 μg/mL for our functionalization protocol.

We then tested whether the antibody concentrations inferred from immunofluorescence are consistent with cell capture. We captured LNCaP cells flowed through a microfluidic device with Hele-Shaw geometry and characterized the cell density as a function of local shear and antibody incubation concentration. Cell capture increased with increasing antibody concentration, as demonstrated in Fig. 3, until the surface becomes saturated with the antibody; these results are in congruence with the immunofluorescence data. As expected, cell capture is more prominent at low shear stress.

Given that 10 μg/mL antibody provides saturation-level cell capture in this system, we then investigated two antibodies and their combination to determine the optimal surface to use for PSMA+ cell capture. To measure the relative ability of different antibodies and antibody mixtures to capture PSMA-positive cells, we captured LNCaPs with two different monoclonal antibodies and a mixture of the two at constant antibody incubation concentration. Figure 4 shows the relative performance of biotinylated-J591, biotinylated-J415, and a 50/50 mixture of biotinylated-J591 with biotinylated-J415 on capture of LNCaPs. In all cases, 10 μg/mL antibody solutions were used when functionalizing the surfaces. Similarly, the capture of LNCaP cells decreases as a function of increasing shear stress, as expected. Over the range of shear stresses measured, captured cell density of the J415 and J415-J591 mixture were both significantly lower ($p<$ 0.001) relative to J591 but not significantly different from one another.

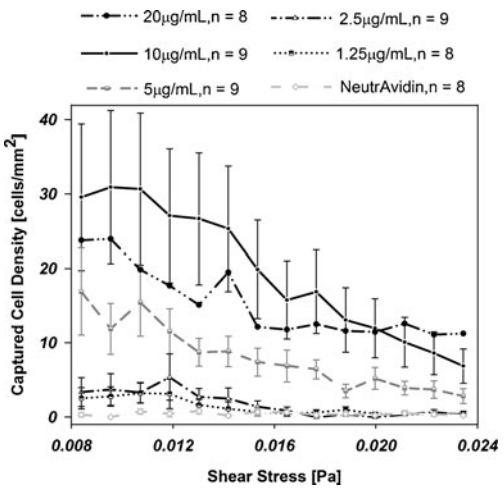

Fig. 3 Cell adhesion to a biotinylated-J591 immunocoated substrate at varying antibody concentrations: 10 (n=9), 5 (n=9), 2.5 (n=9), and 1.25 μg/mL (n=8), as a function of shear stress. Error bars represent the standard error of the mean; error bars are omitted from 20 microgram data for clarity

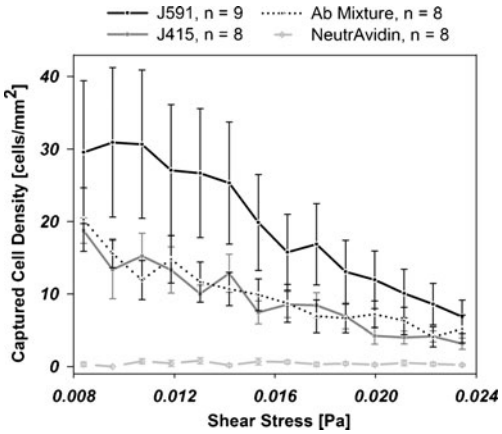

Fig. 4 Cell adhesion to an immunocoated substrate coated with biotinylated-J591 (n=9), -J415 (n=8), a 50/50 mixture of J591/J415 (n=8), and NeutrAvidin (n=8), as a function of local shear stress, as indicated. Error bars denote the standard error of the mean

4 Discussion

Although EpCAM is ubiquitous as an immunoenrichment antigen for CTCs (Nagrath et al. 2007; Shaffer et al. 2007; Olmos et al. 2009; Stott et al. 2010a,b), uncertainties remain regarding the biases introduced by EpCAM capture and EMT (Danila et al. 2011). The expression of PSMA in PCa affords a new transmembrane protein that may be targeted for isolation of circulating prostate cells (Davis et al. 2005). PSMA is expressed exclusively in prostate tissues, with the exception of some neovascular endothelia—e.g., renal cell carcinoma, breast cancer, gastric adenocarcinoma, and colorectal adenocarcinoma (Silver et al. 1997; Chang et al. 1999b; Haffner et al. 2009). PSMA is also expressed at 100–1000-fold lower levels in small intestine, proximal renal tubules, salivary glands, and some astrocytes; these cell types are generally separated from the circulation by epithelial tight junctions, basement layers, or the blood-brain barrier (Horoszewicz et al. 1987; Israeli et al. 1994a, b; Trover et al. 1995; Liu et al. 1997; Silver et al. 1997; Sokoloff et al. 2000; Rajasekaran et al. 2005). These cell types are not expected in circulation.

The anti-PSMA antibodies J591 and J415 are known to target prostate cancer cells in immunotherapeutic studies and are examined in this study to quantify capture performance of PSMA-expressing cells (Smith-Jones et al. 2000; Bander et al. 2003). PSMA exhibits three unique extracellular domains including a protease domain, an apical domain, and a C-terminal domain; all present opportunities for immunocapture (Mesters et al. 2006). J591 and J415 bind to unique external epitopes on the PSMA protein (Liu et al. 1997; Chang et al. 1999a), but published data differs on their competitive nature (Liu et al. 1997; Smith-Jones et al. 2000). As observed from Fig. 4, the performance of J591 is superior for capture compared to J415 at all shear stresses

tested ($p<0.001$). This may be explained by differences in competition for binding at a wall with an antigen location near the cell membrane, as is the case with J415, as compared to one at the apical domain, as with J591 (Liu et al. 1997; Bander et al. 2003; Davis et al. 2005). Although these antibodies bind to distinct locations on the PSMA protein, there are no observed synergistic effects from a surface functionalized with a J591-J415 mixture treatment. Instead, a decreased performance as compared to the standard 10 μg/mL J591 treatment resulted. This mixture performed similarly to a 5 μg/mL J591 treatment. This result is consistent with steric hindrance of simultaneous access of wall-bound antibodies to apical and C-terminal domains of PSMA.

Measured saturation concentrations are in congruence with current standards for microdevice immunocapture. 10–20 μg/mL is a common concentration used for surface functionalization (Gleghorn et al. 2010; Stott et al. 2010a), and in this study, this concentration matches optimal performance in both immunofluorescence and cell capture with minimal reagent use in this study.

The implemented microdevice facilitates simple data harvesting as a result of well-defined local shear stresses on surfaces that can be easily imaged. This platform enables the investigation of the effects of shear stress on the integrity and viability of immobilized cells; factors that must also be considered when designing microdevices for high capture efficiency and capture population purity. The shear stress range examined can be tuned to match any microfluidic immunocapture platform of interest; thus, predictions about cell isolation can be experimentally derived before design and implementation of novel immunocapture devices (Usami et al. 1993).

5 Conclusions

This work characterizes PSMA+ cell capture on J591- and J415- functionalized surfaces as well as surfaces with a combination of these antibodies. J591 performed better than J415 or a combination of J591 and J415 at equal mass concentrations. Immunofluorescence characterization of surface antibody density echoed cell capture rates. Cell capture rates decrease with increasing shear stress. Anti-PSMA rare cell capture gives the potential to enrich prostate cancer circulating tumor cells without biases associated with epithelial-to-mesenchymal transitions.

Acknowledgements The work described was partially supported by the Cornell Center on the Microenvironment & Metastasis through Award Number U54CA143876 from the National Cancer Institute, the Cornell NSF GK-12 program and the Cornell-Sloan Fellowship (S.S.). The authors thank LJ Bonassar for use of the plate reader.

References

W.J. Allard, J. Matera et al., Tumor cells circulate in the peripheral blood of all major carcinomas but not in healthy subjects or patients with nonmalignant diseases. Clin. Cancer Res. **10**(20), 6897–6904 (2004)

H.J.K. Ananias, M.C. van den Heuvel et al., Expression of the gastrin-releasing peptide receptor, the prostate stem cell antigen and the prostate-specific membrane antigen in lymph node and bone metastases of prostate cancer. Prostate **69** (10), 1101–1108 (2009)

N.H. Bander, D.M. Nanus et al., Targeted systemic therapy of prostate cancer with a monoclonal antibody to prostate-specific membrane antigen. Semin. Oncol. **30**(5), 667–676 (2003)

S.S. Chang, D.S. O'Keefe et al., Prostate-specific membrane antigen is produced in tumor-associated neovasculature. Clin. Cancer Res. **5** (10), 2674–2681 (1999a)

S.S. Chang, V.E. Reuter et al., Five different anti-Prostate-specific Membrane Antigen (PSMA) antibodies confirm PSMA expression in tumor-associated neovasculature. Cancer Res. **59**(13), 3192–3198 (1999b)

S.J. Cohen, C.J.A. Punt et al., Relationship of circulating tumor cells to tumor response, progression-free survival, and overall survival in patients with metastatic colorectal cancer. J. Clin. Oncol. **26**(19), 3213–3221 (2008)

F.A.W. Coumans, C.J.M. Doggen et al., All circulating EpCAM+CK +CD45- objects predict overall survival in castration-resistant prostate cancer. Ann. Oncol. **21**(9), 1851–1857 (2010)

D.C. Danila, G. Heller et al., Circulating tumor cell number and prognosis in progressive castration-resistant prostate cancer. Clin. Cancer Res. **13**(23), 7053–7058 (2007)

D.C. Danila, M. Fleisher et al., Circulating tumor cells as biomarkers in prostate cancer. Clin. Cancer Res. **17**(12), 3903–3912 (2011)

M.I. Davis, M.J. Bennett et al., Crystal structure of prostate-specific membrane antigen, a tumor marker and peptidase. Proc. Natl. Acad. Sci. U. S. A. **102**(17), 5981–5986 (2005)

J.S. de Bono, H.I. Scher et al., Circulating tumor cells predict survival benefit from treatment in metastatic castration-resistant prostate cancer. Clin. Cancer Res. **14**(19), 6302–6309 (2008)

J.P. Gleghorn, E.D. Pratt et al., Capture of circulating tumor cells from whole blood of prostate cancer patients using geometrically enhanced differential immunocapture (GEDI) and a prostate-specific antibody. Lab Chip **10**(1), 27–29 (2010)

J. Gostner, D. Fong et al., Effects of EpCAM overexpression on human breast cancer cell lines. BMC Cancer **11**(1), 45 (2011)

A. Gradilone, C. Raimondi, et al. Circulating tumor cells lacking cytokeratin in breast cancer: the importance of being mesenchymal. J. Cell. Mol. Med. (2011): no-no.

M.C. Haffner, I.E. Kronberger et al., Prostate-specific membrane antigen expression in the neovasculature of gastric and colorectal cancers. Hum. Pathol. **40**(12), 1754–1761 (2009)

J.S. Horoszewicz, E. Kawinski et al., Monoclonal antibodies to a new antigenic marker in epithelial prostatic cells and serum of prostatic cancer patients. Anticancer Res. **7**(5B), 927–935 (1987)

R.S. Israeli, W.H. Miller et al., Sensitive tumor cells: comparison of prostate-specific membrane antigen and prostate-specific antigen-based assays. Cancer Res. **54**(24), 6306–6310 (1994a)

R.S. Israeli, C.T. Powell et al., Expression of the prostate-specific membrane antigen. Cancer Res. **54**(7), 1807–1811 (1994b)

B.J. Kirby, A.R. Wheeler et al., Programmable modification of cell adhesion and zeta potential in silica microchips. Lab Chip **3**(1), 5–10 (2003)

R.T. Krivacic, A. Ladanyi et al., A rare-cell detector for cancer. Proc. Natl. Acad. Sci. U. S. A. **101**(29), 10501–10504 (2004)

T. Kusumi, T. Koie et al., Immunohistochemical detection of carcinoma in radical prostatectomy specimens following hormone therapy. Pathol. Int. **58**(11), 687–694 (2008)

H. Liu, P. Moy et al., Monoclonal antibodies to the extracellular domain of prostate-specific membrane antigen also react with tumor vascular endothelium. Cancer Res. **57**(17), 3629–3634 (1997)

S. Maheswaran, D.A. Haber, Circulating tumor cells: a window into cancer biology and metastasis. Curr. Opin. Genet. Dev. **20**(1), 96–99 (2010)

S. Mannweiler, P. Amersdorfer et al., Heterogeneity of Prostate-Specific Membrane Antigen (PSMA) expression in prostate carcinoma with distant metastasis. Pathol. Oncol. Res. **15**(2), 167–172 (2009)

M. Mego, U. De Giorgi et al., Circulating tumor cells in metastatic inflammatory breast cancer. Ann. Oncol. **20**(11), 1824–1828 (2009)

J.R. Mesters, C. Barinka et al., Structure of glutamate carboxypeptidase II, a drug target in neuronal damage and prostate cancer. EMBO J. **25**(6), 1375–1384 (2006)

S. Minner, C. Wittmer et al., High level PSMA expression is associated with early PSA recurrence in surgically treated prostate cancer. Prostate **71**(3), 281–288 (2011)

J.G. Moreno, M.C. Miller et al., Circulating tumor cells predict survival in patients with metastatic prostate cancer. Urology **65**(4), 713–718 (2005)

M. Munz, P.A. Baeuerle et al., The emerging role of EpCAM in cancer and stem cell signaling. Cancer Res. **69**(14), 5627–5629 (2009)

G.P. Murphy, A.-A.A. Elgamal et al., Current evaluation of the tissue localization and diagnostic utility of prostate specific membrane antigen. Cancer **83**(11), 2259–2269 (1998)

S.K. Murthy, A. Sin et al., Effect of flow and surface conditions on human lymphocyte isolation using microfluidic chambers. Langmuir **20**(26), 11649 (2004)

S. Nagrath, L.V. Sequist et al., Isolation of rare circulating tumour cells in cancer patients by microchip technology. Nature **450**(7173), 1235–1239 (2007)

D. Olmos, H.T. Arkenau et al., Circulating tumour cell (CTC) counts as intermediate end points in castration-resistant prostate cancer (CRPC): a single-centre experience. Ann. Oncol. **20**(1), 27–33 (2009)

K. Pantel, C. Alix-Panabières, Circulating tumour cells in cancer patients: challenges and perspectives. Trends Mol. Med. **16**(9), 398–406 (2010)

S. Perner, M.D. Hofer et al., Prostate-specific membrane antigen expression as a predictor of prostate cancer progression. Hum. Pathol. **38**(5), 696–701 (2007)

E.D. Pratt, C. Huang et al., Rare cell capture in microfluidic devices. Chem. Eng. Sci. **66**(7), 1508–1522 (2011)

A.K. Rajasekaran, G. Anilkumar et al., Is prostate-specific membrane antigen a multifunctional protein? Am. J. Physiol. Cell Physiol. **288**(5), C975–C981 (2005)

S. Riethdorf, K. Pantel, Advancing personalized cancer therapy by detection and characterization of circulating carcinoma cells Circulating tumor cells in cancer patients Riethdorf & Pantel. Ann. N. Y. Acad. Sci. **1210**(1), 66–77 (2010)

J.S. Ross, C.E. Sheehan et al., Correlation of primary tumor prostate-specific membrane antigen expression with disease recurrence in prostate cancer. Clin. Cancer Res. **9**(17), 6357–6362 (2003)

H.I. Scher, X. Jia et al., Circulating tumour cells as prognostic markers in progressive, castration-resistant prostate cancer: a reanalysis of IMMC38 trial data. Lancet Oncol. **10**(3), 233–239 (2009)

D.R. Shaffer, M.A. Leversha et al., Circulating tumor cell analysis in patients with progressive castration-resistant prostate cancer. Clin. Cancer Res. **13**(7), 2023–2029 (2007)

S. Shiah, K. Tai et al., Epigenetic regulation of EpCAM in tumor invasion and metastasis. J. Canc. Mol. **3**, 165–168 (2008)

D.A. Silver, I. Pellicer et al., Prostate-specific membrane antigen expression in normal and malignant human tissues. Clin. Cancer Res. **3**(1), 81–85 (1997)

A. Sin, S.K. Murthy et al., Enrichment using antibody-coated microfluidic chambers in shear flow: model mixtures of human lymphocytes. Biotechnol. Bioeng. **91**(7), 816–826 (2005)

P.M. Smith-Jones, S. Vallabahajosula et al., *In vitro* characterization of radiolabeled monoclonal antibodies specific for the extracellular domain of prostate-specific membrane antigen. Cancer Res. **60** (18), 5237–5243 (2000)

R.L. Sokoloff, K.C. Norton et al., A dual-monoclonal sandwich assay for prostate-specific membrane antigen: levels in tissues, seminal fluid and urine. Prostate **43**(2), 150–157 (2000)

S.L. Stott, C.-H. Hsu et al., Isolation of circulating tumor cells using a microvortex-generating herringbone-chip. Proc. Natl. Acad. Sci. **107**(43), 18392–18397 (2010a)

S.L. Stott, R.J. Lee et al., Isolation and characterization of circulating tumor cells from patients with localized and metastatic prostate cancer. Sci. Transl. Med. **2**(25), 25ra23 (2010b)

S.D. Sweat, A. Pacelli et al., Prostate-specific membrane antigen expression is greatest in prostate adenocarcinoma and lymph node metastases. Urology **52**(4), 637–640 (1998)

J.K. Trover, M.L. Beckett et al., Detection and characterization of the prostate-specific membrane antigen (PSMA) in tissue extracts and body fluids. Int. J. Cancer **62**(5), 552–558 (1995)

S. Usami, H.H. Chen et al., Design and construction of a linear shear stress flow chamber. Ann. Biomed. Eng. **21**(1), 77–83 (1993)

G.L. Wright, C. Haley et al., Expression of prostate-specific membrane antigen in normal, benign, and malignant prostate tissues. Urol. Oncol. **1**(1), 18–28 (1995)

J.G.L. Wright, B. Mayer Grob et al., Upregulation of prostate-specific membrane antigen after androgen-deprivation therapy. Urology **48**(2), 326–334 (1996)